

Bone Density Development of the Temporal Bone Assessed by Computed Tomography

Kuniyuki Takahashi, Yuka Morita, Shinsuke Ohshima, Shuji Izumi, Yamato Kubota, and Arata Horii

Department of Otolaryngology Head and Neck Surgery, Niigata University Faculty of Medicine, Niigata, Japan

Hypothesis: The temporal bone shows regional differences in bone development.

Background: The spreading pattern of acute mastoiditis shows age-related differences. In infants, it spreads laterally and causes retroauricular swelling, whereas in older children, it tends to spread medially and causes intracranial complications. We hypothesized that bone maturation may influence the spreading pattern of acute mastoiditis.

Methods: Eighty participants with normal hearing, aged 3 months to 42 years, participated in this study. Computed tomography (CT) values (Hounsfield unit [HU]) in various regions of the temporal bone, such as the otic capsule (OC), lateral surface of the mastoid cavity (LS), posterior cranial fossa (PCF), and middle cranial fossa (MCF), were measured as markers of bone density. Bone density development curves, wherein CT values were plotted against age, were created for each region. The age at which the CT value

exceeded 1000HU, which is used as an indicator of bone maturation, was calculated from the development curves and compared between the regions.

Results: The OC showed mature bone at birth, whereas the LS, PCF, and MCF showed rapid maturation in early childhood. However, there were significant regional differences in the ages of maturation: 1.7, 3.9, and 10.8 years for the LS, PCF, and MCF, respectively.

Conclusion: To our knowledge, this is the first report to show regional differences in the maturation of temporal bone, which could partly account for the differences in the spreading pattern of acute mastoiditis in individuals of different ages. **Key Words:** Bone density—CT value—Development—Temporal bone.

Otol Neurotol 38:1445–1449, 2017.

Skeletal bones show dynamic changes in morphometric and compositional characteristics with age. Bone mineral density (BMD) is generally low at birth and increases with age. However, there are differences in BMD development among the extremities, spine, and cranial bones (1,2). Developmental differences in bone density can also be observed among regions within the cranial bones (3). We hypothesized that such regional differences in bone density development may affect the pathophysiology of infectious diseases of the temporal bone.

The structural characteristics of the temporal bone are different from those of other bones. Other skeletal bones are generally sterile, but the temporal bone is more susceptible to bacterial infection because the pneumatized cavity in the temporal bone connects to the nasopharyngeal cavity via the Eustachian tube. The pneumatized cavity also faces the intracranial space.

Thin cortical bones separate the pneumatized cavity from the surrounding important structures, thereby acting as a barrier to control the spread of infection. Niv et al. (4) reported that a retroauricular swelling was observed in 77% of patients with acute mastoiditis under 1 year of age, whereas a significantly lower number of patients over 3 years of age (42%) developed a retroauricular swelling with acute mastoiditis. This report suggests that acute mastoiditis spreads laterally, causing retroauricular swelling in infants, and medially, causing intracranial complications in older children. In the present study, we hypothesized that the regional differences in bone maturation of the temporal bone may influence the spreading pattern of acute mastoiditis.

To measure BMD of the spine and extremities, dual x-ray absorptiometry (DXA) is usually used. Quantitative computed tomography (qCT), in which a calibrating phantom is used, is an alternative to measure BMD (5). It has been shown in the recent past that CT values (Hounsfield Units [HU]) obtained from clinical CT (6) and qCT may be used to evaluate BMD. However, qCT is now being replaced by clinical CT for assessing BMD (2,3,7,8). Therefore, in the present study, we used CT values to measure BMD.

In the present study, we investigated the age of bone maturation of different regions of the temporal bone,

Address correspondence and reprint requests to Kuniyuki Takahashi, M.D., Department of Otolaryngology, Niigata University Faculty of Medicine, 1 Asahi-machi, Chuo-ku, Niigata 951-8510, Japan; E-mail: kuniyuki@med.niigata-u.ac.jp

The authors have no conflict of interest directly relevant to the content of this article.

DOI: 10.1097/MAO.0000000000001566

such as the otic capsule (OC), lateral surface of the mastoid cavity (LS), posterior cranial fossa (PCF), and middle cranial fossa (MCF) by evaluating CT values obtained from clinical CT of ears with no hearing impairment.

MATERIALS AND METHODS

This study was conducted with the approval of the Institutional Review Board of the Niigata University (approval number #2016-0080).

High-resolution temporal bone CT images taken at our hospital in sequential years were retrospectively reviewed. Although CT images were obtained to identify the cause of hearing loss or to assess the temporal bone pathology, we only evaluated healthy ears with normal hearing in this study. The criteria for normal hearing included ears that had passed the newborn hearing screening, had a threshold of less than 40 dB on auditory brainstem response (ABR) or an average threshold of less than 20 dB on pure-tone audiometry at 0.5, 1, and 2 kHz. Patients showing developmental delay or congenital anomalies were excluded from the study. The study included only patients under 44 years of age with no osteoporotic changes due to aging, to allow an accurate evaluation of density development (9). Accordingly, 80 ears from 50 men and 30 women participants, ranging in age between 3 months and 42 years, were included in this study. Fifty-nine ears were included from participants under 20 years of age and 21 ears from participants over 20 years of age.

Digital Imaging and Communications in Medicine (DICOM) data based on high-resolution (1.0-mm slice) CT scans obtained from the patients were imported into an image analysis software (AquariusNET Server, TeraRecon, Foster City, CA). Three regions of interest (ROIs) were set for each area, including the OC, MCF, PCF, and LS of the mastoid cavity. The three ROIs for the OC were set medial to the basal turn, second turn, and at the apex of the cochlea. The ROIs for MCF, PCF, and LS were distributed at approximately equal distances to each other. The size of each ROI was set as narrow as 0.3 mm^2 to avoid partial volume effects on the CT values (Fig. 1). Large ROIs might contain adjacent air space resulting in low CT values. Analysis was performed on axial slice images. If the cortical bone was thick, we set the ROI at the border of the medial surface in the cortical bone. The CT values of the three ROIs were averaged to evaluate the bone density of each region, which was plotted against age. To assess the association between CT values and age, we used the Spearman's rank test and calculated the ρ correlation coefficient and p value. We used a standard scale to rank the Spearman's ρ coefficient: less than 0.2 was regarded as negligible correlation, 0.2 to 0.4 as low correlation, 0.4 to 0.7 as moderate correlation, and 0.7 to 1.0 as high correlation. If the Spearman's test was statistically significant, a regression analysis was performed with the CT value as the dependent variable and age as the independent variable. The data were also evaluated using a one-way analysis of covariance (ANCOVA), designed to test the relative effect of the regions on the dependent variables, controlling possible interaction and the confounding influence of age as a continuous predictor variable. Before this analysis, the homogeneity of variance assumption was tested and found valid using the Levene's test ($p < 0.05$). Post-hoc comparison was performed using Bonferroni correction. p values < 0.05 were considered statistically significant. All data were analyzed using SPSS statistics version 21 (IBM, Armonk, NY).

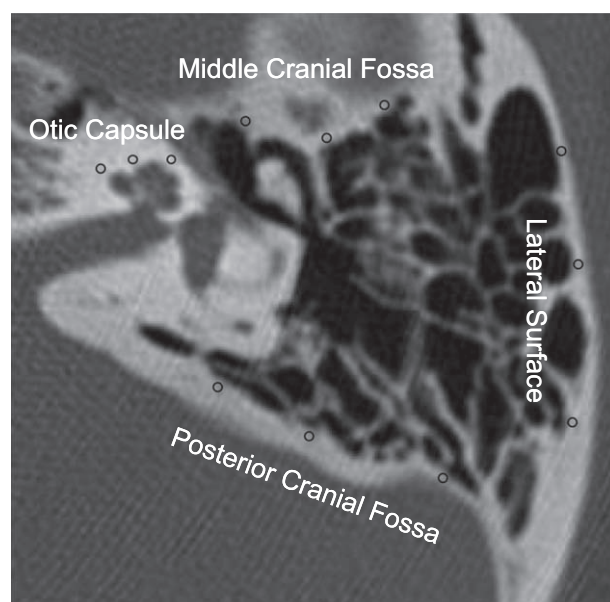


FIG. 1. Example of region of interest (ROI) setting. In the axial images, three ROIs are manually set for each region (open circles). The area of each ROI is 0.3 mm^2 .

RESULTS

The OC was already mature ($> 1000\text{ HU}$) at birth and the bone density was found to remain constant until adulthood ($2009 \pm 63.9\text{ HU}$, mean \pm SD). Therefore, the Spearman's rank test showed no significant correlation between CT values and age ($p > 0.05$, $\rho = 0.002$) for OC. In contrast, the test showed a high correlation between CT values and age, for other regions. The correlations were highly significant ($p < 0.01$, $\rho = 0.927$ in LS; $p < 0.01$, $\rho = 0.885$ in PCF; and $p < 0.01$, $\rho = 0.717$ in MCF). The regression analysis performed subsequently showed that CT values of the LS, PCF, and MCF consistently followed a logarithmic curve and the coefficients of determination R^2 for the LS, PCF, and MCF were 0.880, 0.792, and 0.577, respectively (Fig. 2B–D).

Because the CT values of most cortical bones in the extremities of adults were over 1000 HU (10), 1000 HU was considered the indicator of cortical bone maturation. Whereas CT value of the OC was approximately 2000 HU at birth, the ages at which the CT values of the LS, PCF, and MCF reached 1000 HU were 1.7, 3.9, and 10.8 years, respectively (Fig. 3). ANCOVA showed a statistically significant effect ($p < 0.001$) of the regions on CT values, and the post-hoc test also showed significant differences in all comparisons ($p < 0.05$ for MCF versus PCF; $p < 0.01$ for MCF versus LS and PCF versus LS).

The representative CT findings at the age of 3 months, 3 years and 6 months, and 19 years and 8 months are presented in Figure 4. As shown in this figure, regional differences in bone density development, as indicated in Figure 3, can be visually recognized.

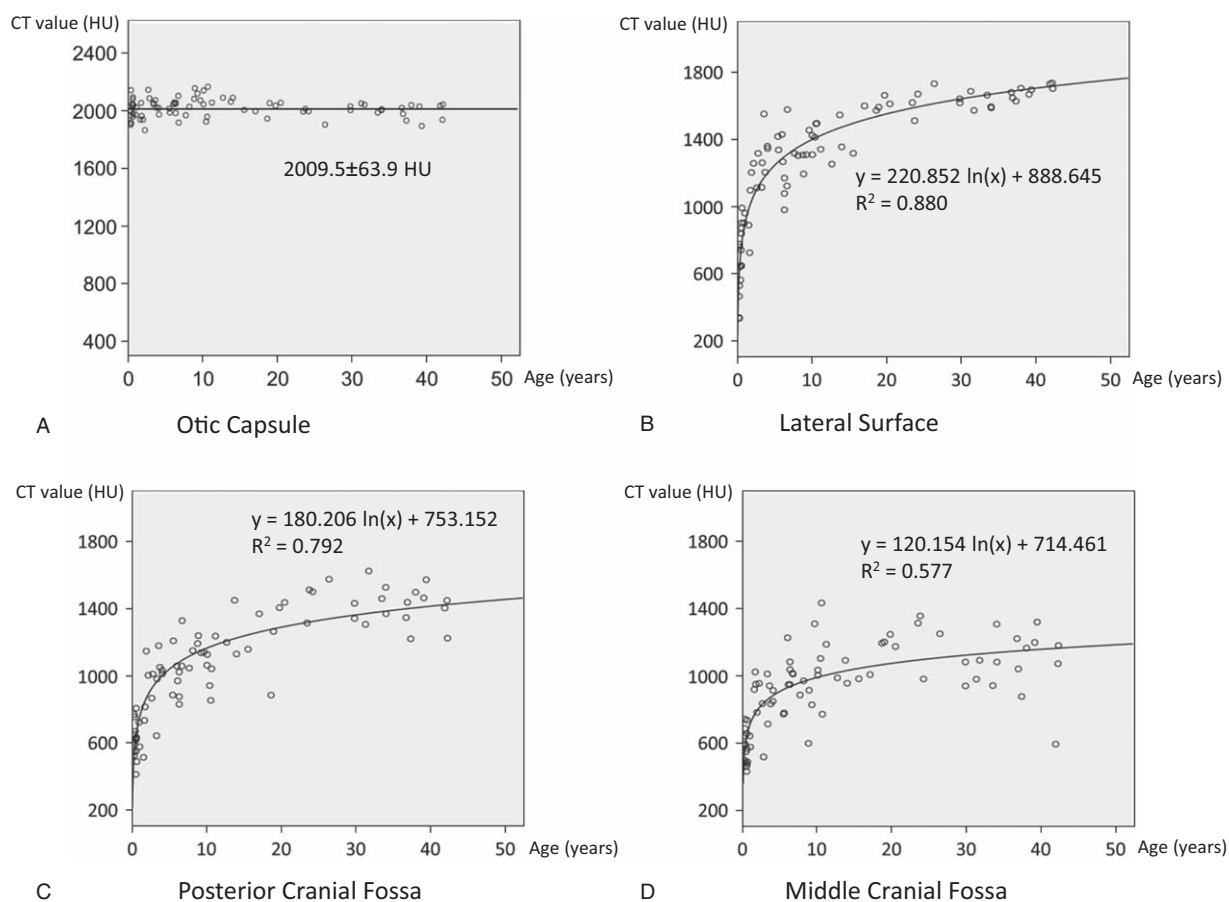


FIG. 2. Bone density development curves for the otic capsule (OC) (A), lateral surface (LS) (B), posterior cranial fossa (PCF) (C), and middle cranial fossa (MCF) (D). The CT values of each region are plotted against age. The bone density of the OC is high at birth and remains constant until adulthood (A). The CT values of the LS, PCF, and MCF are significantly correlated with age, following a logarithmic curve (B–D). The correlation coefficients for the LS, PCF, and MCF are 0.880, 0.792, and 0.577, respectively. CT indicates computed tomography.

DISCUSSION

To our knowledge, this is the first report to describe the regional differences in the development of bone density of the temporal bone. Previous studies have focused mainly on the development of mastoid air cells (11,12). The present results prove that OC is already mature at birth and that the bone density remains constant until adulthood (Fig. 3). Consistent with the findings of previous reports (13), CT value of the OC was found to be as high as 2000 HU (much higher than that of other regions of the temporal bone). The bone density in other regions of the temporal bone developed rapidly during early childhood. However, there were significant regional differences. The earliest maturation was observed in LS followed by PCF and MCF (Fig. 3). The bone density development followed a logarithmic curve (Fig. 2B–D) and was similar to bone density development in parts of other cranial bones, such as the frontal, parietal, and occipital bones (2). Bone density development paralleled the increase in head circumference as well as increase in the skull breadth, length, and height (14). The R^2 correlation index between bone density and age was 0.880,

0.792, and 0.577 in the LS, PCF, and MCF, respectively (Fig. 2B–D). Although statistically significant, the R^2 value for MCF was relatively smaller than that for LS and

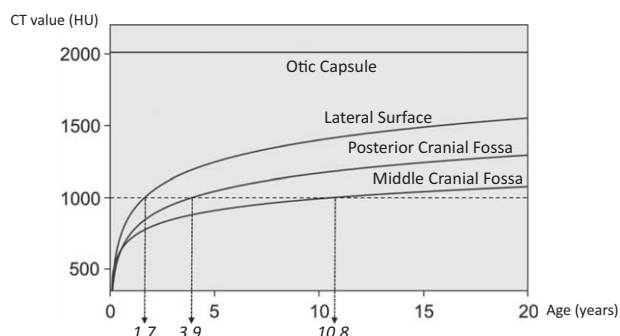


FIG. 3. Comparison of bone density development curves of different regions in the temporal bone. Bone density of the otic capsule is constant. However, bone densities of other regions increase rapidly in early childhood. The age at which the CT value reaches 1000 HU, which is used as an indicator of bone maturation, is 1.7 years for the lateral surface, 3.9 years for the posterior cranial fossa, and 10.8 years for the middle cranial fossa. CT indicates computed tomography.

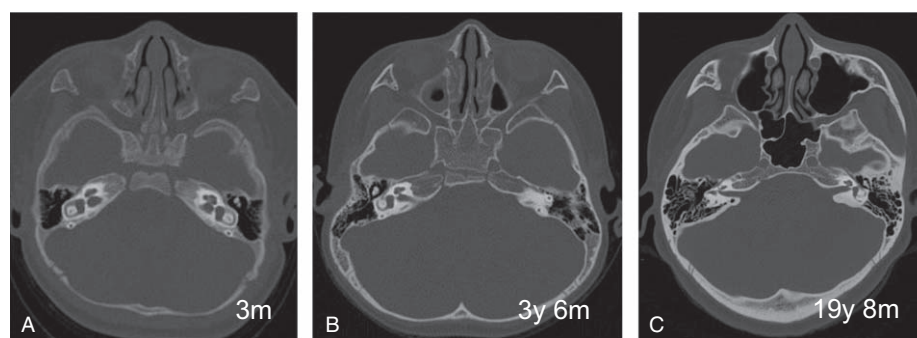


FIG. 4. CT images at different ages. CT images at the age of 3 months (A), 3 years and 6 months (B), and 19 years and 8 months (C). The window level is 1000 HU and the window width is 4000 HU in all images. The otic capsule appears conspicuous in A. The bone density of the cranial bone, except for the otic capsule, increases with age. CT indicates computed tomography.

PCF. This was probably because the ROI for MCF may have included pixels of cancellous bone, periosteal surface, or aerated cells in addition to the compact bone; moreover, the measurement points of MCF were arranged in a tangential direction on the axial slice of CT, which resulted in partial volume effect of CT.

Consistent with the results of CT value measurements, we could visually recognize the conspicuous OC on the CT scan of an infant (Fig. 4A). We assumed that regional differences in bone density development might be causally related to the differences in spreading pattern of acute mastoiditis according to age. With respect to the presence or absence of intracranial complications in acute mastoiditis, retroauricular subperiosteal abscess was significantly more common in infants than in older children (4). The results of the present study demonstrate that all regions except the OC are immature in young children, and that the LS matures earlier than the PCF and MCF. Therefore, a mastoid cavity infection in young children can potentially spread along any direction. However, the infection may not spread laterally in older children because of early maturation of LS. Consequently, the infection may tend to spread medially in older children, leading to intracranial complications. In addition to the regional differences in bone density development, pneumatization, bone thickness, and other factors of the temporal bone should be considered factors that influence the spreading pattern of acute mastoiditis.

Similar to the temporal bone, the bones of the nasal cavity are also pneumatized and susceptible to bacterial infection. With respect to the complications of acute rhinosinusitis, orbital complications were significantly more common than intracranial complications in young patients (15). These age-dependent differences in spreading patterns of infection in both acute mastoiditis and acute rhinosinusitis may be partly accounted for by regional differences in bone density development.

CONCLUSIONS

To our knowledge, this is the first study to report bone density development of normal temporal bone using CT. The bone of the OC was already mature at birth,

with a bone density of more than 1000 HU. Whereas the bone density of the MCF, PCF, and LS developed rapidly in early childhood, there were significant regional differences in bone density development; earliest maturation was observed in LS followed by PCF and MCF. These regional differences in bone maturation could partly account for the difference in spreading pattern of acute mastoiditis observed in patients of different ages.

Acknowledgments: This study was presented at 52nd Annual Spring Meeting for American Neurotology Society 2017 at San Diego.

REFERENCES

1. Lee SH, Desai SS, Shetty G, et al. Bone mineral density of proximal femur and spine in Korean children between 2 and 18 years of age. *J Bone Miner Metab* 2007;25:423–30.
2. Delye H, Clijmans T, Mommaerts MY, et al. Creating a normative database of age-specific 3D geometrical data, bone density, and bone thickness of the developing skull: a pilot study. *J Neurosurg Pediatr* 2015;16:687–702.
3. Smith K, Politte D, Reiker G, et al. Automated measurement of pediatric cranial bone thickness and density from clinical computed tomography. *Conf Proc IEEE Eng Med Biol Soc* 2012;2012:4462–5.
4. Niv A, Nash M, Slovik Y, et al. Acute mastoiditis in infancy: the Soroka experience: 1990–2000. *Int J Pediatr Otorhinolaryngol* 2004;68:1435–9.
5. Mazonakis M, Damilakis J. Computed tomography: what and how does it measure? *Eur J Radiol* 2016;85:1499–504.
6. Pickhardt PJ, Pooler BD, Lauder T, et al. Opportunistic screening for osteoporosis using abdominal computed tomography scans obtained for other indications. *Ann Intern Med* 2013;158:588–95.
7. Schreiber JJ, Anderson PA, Hsu WK. Use of computed tomography for assessing bone mineral density. *Neurosurg Focus* 2014;37:E4.
8. Link TM, Koppers BB, Licht T, et al. In vitro and in vivo spiral CT to determine bone mineral density: initial experience in patients at risk for osteoporosis. *Radiology* 2004;231:805–11.
9. Orimo H, Hayashi Y, Fukunaga M, et al. Diagnostic criteria for primary osteoporosis: year 2000 revision. *J Bone Miner Metab* 2001;19:331–7.
10. Ciarelli MJ, Goldstein SA, Kuhn JL, et al. Evaluation of orthogonal mechanical properties and density of human trabecular bone from the major metaphyseal regions with materials testing and computed tomography. *J Orthop Res* 1991;9:674–82.
11. Cinamon U. The growth rate and size of the mastoid air cell system and mastoid bone: a review and reference. *Eur Arch Otorhinolaryngol* 2009;266:781–6.

12. Rubensohn G. Mastoid pneumatization in children at various ages. *Acta Otolaryngol* 1965;60:11-4.
13. Kawase S, Naganawa S, Sone M, et al. Relationship between CT densitometry with a slice thickness of 0.5 mm and audiometry in otosclerosis. *Eur Radiol* 2006;16:1367-73.
14. Dekaban AS. Tables of cranial and orbital measurements, cranial volume, and derived indexes in males and females from 7 days to 20 years of age. *Ann Neurol* 1977;2:485-91.
15. Oxford LE, McClay J. Complications of acute sinusitis in children. *Otolaryngol Head Neck Surg* 2005;133:32-7.